Electronic Structure of YbB_6: Is it a Topological Insulator or Not?

Chang-Jong Kang,[1] J. D. Denlinger,[2,*] J. W. Allen,[3] Chul-Hee Min,[4] F. Reinert,[4] B. Y. Kang,[5] B. K. Cho,[5] J.-S. Kang,[6] J. H. Shim,[1,7] and B. I. Min[1,†]

[1]*Department of Physics, PCTP, Pohang University of Science and Technology, (POSTECH) Pohang 37673, Korea*
[2]*Advanced Light Source, Lawrence Berkeley Laboratory, Berkeley, California 94720, USA*
[3]*Department of Physics, Randall Laboratory, University of Michigan, Ann Arbor, Michigan 48109, USA*
[4]*Universität Würzburg, Experimentelle Physik VII, 97074 Würzburg, Germany*
[5]*School of Materials Science and Engineering, GIST, Gwangju 61005, Korea*
[6]*Department of Physics, The Catholic University of Korea, Bucheon 14662, Korea*
[7]*Department of Chemistry and Division of Advanced Nuclear Engineering, POSTECH, Pohang 37673, Korea*

(Received 22 August 2015; published 17 March 2016)

To finally resolve the controversial issue of whether or not the electronic structure of YbB_6 is nontrivially topological, we have made a combined study using angle-resolved photoemission spectroscopy (ARPES) of the nonpolar (110) surface and density functional theory (DFT). The flat-band conditions of the (110) ARPES avoid the strong band bending effects of the polar (001) surface and definitively show that YbB_6 has a topologically trivial B $2p$-Yb $5d$ semiconductor band gap of ~0.3 eV. Accurate determination of the low energy band topology in DFT requires the use of a modified Becke-Johnson exchange potential incorporating spin-orbit coupling and an on-site Yb $4f$ Coulomb interaction U as large as 7 eV. The DFT result, confirmed by a more precise GW band calculation, is similar to that of a small gap non-Kondo nontopological semiconductor. Additionally, the pressure-dependent electronic structure of YbB_6 is investigated theoretically and found to transform into a p-d overlap *semimetal* with small Yb mixed valency.

DOI: 10.1103/PhysRevLett.116.116401

A great deal of recent attention has been paid to the topological nature of strongly correlated systems, which include the topological Mott insulator [1,2], the fractional topological insulator [3,4], and the topological Kondo insulator (TKI) [5]. In these systems, the interplay between topological characteristics and strong electron correlations provides new interesting phenomena that can possibly be utilized for spintronic and quantum computing applications.

The first candidate material for a TKI is SmB_6, which has been predicted first theoretically [5–8], and then studied intensively by transport [9–11], angle-resolved photoemission spectroscopy (ARPES) [12–15], and scanning tunneling microscopy or spectroscopy (STM/STS) [16,17] experiments to explore its surface states. Subsequently, other $4f$-electron systems have been proposed as TKIs and topological Kondo semimetals [18–24]. Two essential common ingredients for a nontrivial topological character are (i) band inversion between opposite parity $4f$ and $5d$ states, caused by rare-earth mixed valence, and (ii) a large spin-orbit coupling (SOC) provided by the $4f$ states. At the simplest level a strongly correlated bulk topological insulator (TI) would have the generic TI property of protected, symmetry-required, spin-textured metallic Dirac cone surface states that span the insulating bulk gap.

YbB_6 of our present interest was proposed to be a TKI with the mixed-valence state of Yb being 2.2 ($n_f = 13.8$) based on the inverted Yb $4f$-$5d$ bands obtained in the density-functional theory (DFT) + Gutzwiller band method [22]. However, early photoemission [25] and recent ARPES [26–29] show that the binding energy (BE) of the Yb $4f_{7/2}$ band is about 1 eV, indicating that there would be no f-d band inversion and so YbB_6 would not be a TKI. Then, inspired by the observation of (001) surface states having the appearance of Dirac cones [26–28], two ARPES groups proposed that YbB_6 would be a weakly correlated TI with band inversion between opposite parity Yb $5d$ and B $2p$ bands [27,28]. The topological origin of the observed surface states was questioned [29], however, because they were observed to not follow the expected linear Dirac cone dispersion and to exhibit time-dependent changes. Instead, band bending and surface quantum well confinement arising from the (001) polar surface was suggested, while not explicitly proposing that YbB_6 is not a TI.

The p-d band inversion TI scenario was supported theoretically with DFT + SOC + U ($U = 4$ eV) calculations [27,30], but also with an incorrect 0.3 eV BE of the Yb $4f_{7/2}$ state and in contradiction to an earlier calculation [31] using $U = 7$ eV that obtained a p-d inverted *semimetal* with the correct experimental Yb $4f$ energy. These current experimental and theoretical uncertainties have prevented a consensus on the topological nature of YbB_6.

In this Letter, we report new ARPES experiments that definitively demonstrate the non-Kondo non-TI electronic

structure of YbB_6 and new DFT theory that agrees well with the experimental results and strongly supports the same conclusion. ARPES for the *nonpolar* (110) surface reveals a clear *p*-*d* semiconductor gap with no in-gap surface states, whereas all surfaces of a TI system must have surface states. Calculations incorporating the SOC and U into the modified Becke-Johnson (mBJ) potential [32] describe properly the BE of the Yb $4f_{7/2}$ band and the observed ARPES spectra of a topologically trivial Yb $5d$-B $2p$ band gap. We have also investigated the pressure-dependent electronic structure of YbB_6 and found that the high pressure phase is a topologically nontrivial *p*-*d* overlap *semimetal* with an Yb $4f_{7/2}$ BE of ~0.5 eV, rather than an full insulator. This result explains a recent experimental study of transport and Yb valence under pressure [33].

ARPES measurements were performed at the MERLIN Beam line 4.0.3 at the Advanced Light Source in the photon energy ($h\nu$) range of 30–150 eV. An elliptically polarized undulator was employed, which allows selection of *s* and *p* polarization of the incident light. A Scienta R8000 hemispherical electron energy analyzer was used with energy resolution set to ≈20 meV [34]. Measurements were performed in a vacuum of better than 5×10^{-11} Torr for the sample cooled down to ≈30 K.

The band calculations were performed using the full-potential linearized augmented plane-wave (FLAPW) band method, as implemented in the WIEN2K package [47]. For the DFT calculations, the Perdew-Burke-Ernzerhof exchange-correlation functional was used in the generalized-gradient approximation (GGA). In the GGA+SOC+U method, a correlation energy of $U = 7$ eV was chosen to obtain the correct experimental value of the Yb $4f$ BE of ≈1 eV, which is consistent with the previous calculations [31,48]. The mBJ potential is adopted to provide band gap corrections in agreement with the improved many-body, but much more computation-demanding *GW* calculation [32,49]. The details of the calculational methods are described in the Supplemental Material [34].

For insulating hexaborides, the polarity of (001) surfaces with different charge terminations can lead to *n*- and *p*-type band bending and quantum well states that make it difficult for ARPES to directly observe the bulk band gap. Also, spectra from spatially inhomogeneous regions (i.e., both *n* and *p* type) can falsely appear to show Dirac cones or *p*-*d* overlap [29,50]. While surface modification and aging provide some control over the band bending and assist in the ARPES interpretations [50], these problematic band-bending effects can be avoided by instead measuring a nonpolar surface such as the (110) surface whose charge neutral bulk termination is schematically illustrated in Fig. 1(a). For this purpose, a (110) surface of YbB_6 was prepared from the natural facet of a single crystal grown by the aluminum-flux method. After etching in hydrochloric acid and ion sputtering of the surface, the sample was annealed to 1300°C in ultrahigh vacuum to produce a spatially uniform 1×1 ordered surface [34].

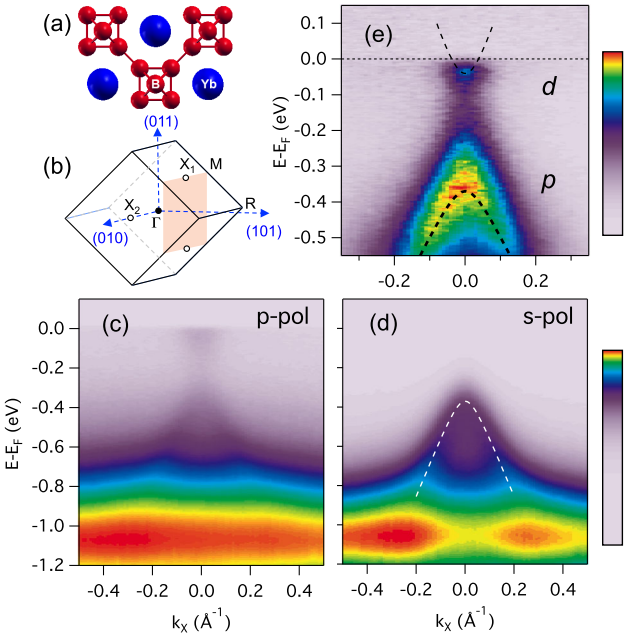

FIG. 1. (a) Schematic structure of the non-polar YbB_6 (110) surface. (b) Cubic BZ with (110) orientation illustrating the locations of bulk X points. (c),(d) X-point spectra measured at $h\nu = 120$ eV with *p* and *s* polarization, illustrating the opposite polarization dependence of *p*-hole and *d*-electron states. (e) Zoom of the *p*-polarization spectrum with the Yb $4f$ spectral intensity removed to enhance the view of the ~0.3 eV band gap. Dashed lines are nonparabolic fits to the spectral intensity maxima (see text).

X-point ARPES spectra measured along $M - X - M$ at $h\nu = 120$ eV using two different linear polarizations of the incident light is shown in Figs. 1(c) and 1(d). Above a strong Yb $4f$ peak at −1.05 eV, the *p*-polarization spectrum shows a weak hole-band dispersion and a small electronlike intensity at E_F. A strong polarization selectivity of these states is revealed by the *s*-polarization spectrum in Fig. 1(d), where the electron conduction state is totally suppressed and the valence hole band is strongly enhanced to manifest a triangularlike dispersion with a rounded-maximum and hybridization interaction with the Yb $4f$ states. The strong hole-band intensity allows a quantitative fit (dashed line) to a two-band $k \cdot p$ nonparabolic dispersion model [34] with a band maximum of 0.35 eV below E_F.

Figure 1(e) shows an enlarged view of the *p*-polarization spectrum in which the Yb $4f$ spectral intensity tail has been divided out to obtain an enhanced image of the ~0.3 eV semiconductor band gap between the B $2p$ valence and Yb $5d$ conduction states. To further characterize the conduction band dispersion and energy minimum, K dosing of the surface was used to induce a small *n*-type band bending until the electron pocket was increased in depth to 0.2 eV,

revealing enough of a dispersion [34] to perform similar nonparabolic dispersion analysis. The resulting process exhibited no discernible surface band gap narrowing, thus allowing evaluation of a band gap of 0.32 eV.

To explicitly confirm that the bands shown in Fig. 1 are bulk, we have measured their k_z dependences in the process of locating the bulk X points. Figures 2(a) and 2(b) show the k_y-k_z maps at fixed $k_x = -0.53$ Å^{-1} for the valence band at -0.3 eV and the conduction band at E_F, respectively. Both constant energy cuts exhibit strong intensity features close to bulk X points at $k_y = 0$ for $h\nu = 76$ and 120 eV as well as intensities at X points of the second Brillouin zone (BZ) at $k_y = \pm 1.5$ Å^{-1}. The small vertical k_z elongation of the X-point intensities in Fig. 2 is well accounted for by the inherent bulk band structure anisotropy (see Fig. 3) and the k_z-broadening effect resulting from the finite inelastic mean free path of the photoelectrons. The pinning of E_F at the bottom of the conduction band is consistent with the negative sign of the bulk Hall coefficient [33,51,52], and consistent with flat-band conditions of the nonpolar (110) surface. Hence, both the valence and conduction bands shown in Fig. 1 are 3D-like bulk bands and do not originate from the 2D-like surface states. The strong polarization dependence in Fig. 1(d) also independently confirms that these states are not linear Dirac cone dispersions, which would instead exhibit some continuity of the same orbital characters between the upper and lower parts of the Dirac cone.

The bulk X-point spectrum in Fig. 1(e) exhibiting a clear small direct semiconductor gap between valence and conduction band states and the absence of in-gap surface states is the central experimental result of this study. The (110) ARPES definitively proves the absence of a p-d overlapping band structure and hence a lack of parity inversion that is the key first requirement for a topological electronic structure interpretation of previous ARPES for the (001) surface. Therefore, the observed chirality in 2D surface states of YbB_6 (001) in circular dichroism (CD)

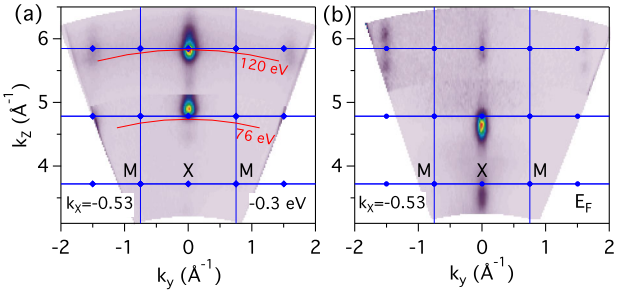

FIG. 2. Off-normal photon-dependent map of YbB_6 (110) at fixed $k_x = -0.53$ Å^{-1}, as shown in Fig. 1(b), of the spectral intensity of (a) valence band at -0.3 eV and (b) conduction band at E_F. The 3D bulklike k_z dependence of both the valence and conduction bands confirms the flat band conditions of the nonpolar (110) surface.

[26] and spin-resolved ARPES [28], cited to support the TI scenario of single-spin in-gap states, must have alternative explanations. Geometrical and final state effects are known to allow the detection of CD and spin polarization in photoemission of nonchiral and nonmagnetic solids [53,54], and can prevent an unambiguous detection of spin-polarization asymmetries in YbB_6, as discussed elsewhere [50].

Next we turn our attention to theoretical predictions of the YbB_6 electronic structure using the DFT method. We first reproduce the literature result [31] of a GGA + SOC + U (7 eV) calculation for YbB_6 in Fig. 3(a), which predicts a semimetallic band structure with a p-d band overlap at E_F. The local gapping at the band crossing points arises from rather weak $5d$ SOC [55]. Since the p-d overlap anticrossing points vary in energy around the X point, the small local gapping cannot produce a full bulk gap, resulting in a complex semimetallic Fermi surface (FS), consisting of "lens" hole and "napkin ring" electron sheets. The calculated YbB_6 $4f$ BE of 0.7–0.8 eV relative to the valence band maximum is in agreement with the experimental ARPES result in Fig. 1 of 1.05 eV which includes the 0.32 eV band gap. The location of the $4f$ state far from E_F results in only a minor influence on the semimetallic FS that is thus very similar to predictions of the non-rare-earth divalent hexaborides [56–58].

In Fig. 3(b), we present an mBJ + SOC + U (7 eV) band result, overlaid with open-core pseudopotential single pass GW band result (dots) [34]. In both cases, the small p-d overlap of the GGA + SOC + U calculation in Fig. 3(a) is transformed into a small ≈0.1 eV semiconductor gap with good quantitative agreement between the two methods

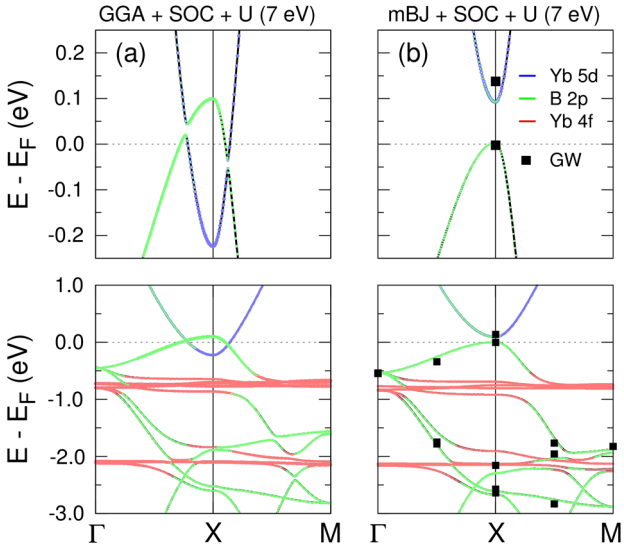

FIG. 3. DFT-Wien2k band structures of YbB_6. (a) GGA+SOC + U (7 eV) calculation yields a semimetallic p-d overlap with anticrossing gaps. (b) mBJ + SOC + U (7 eV) bands overlaid with open-core GW band results (dots). Both exhibit semiconductor band gaps.

[34]. This result clearly indicates that YbB_6 is a topologically trivial small band-gap semiconductor. Not surprisingly, slab calculations for both the YbB_6 (001) and (110) surfaces also show no topological in-gap surface states (see the Supplemental Material [34]).

This semiconductor result is reminiscent of the case of CaB_6, whose early DFT-based semimetallic model for anomalous transport was revised to be that of a 1 eV semiconductor with the assistance of *GW* theory [59], and subsequently confirmed with ARPES [60] and other experiments using high-purity boron samples [61,62]. This straightforward theoretical prediction for YbB_6 of being a topologically trivial semiconductor is in contrast to two recent calculations that predict YbB_6 to be a TI based on f-d band inversion [22] or p-d inversion [27,30]. The flaws in these previous band calculations, resulting in incorrect Yb $4f$ binding energies and mixed valency, are discussed in detail in the Supplemental Material [34], along with angle-integrated valence band spectra from the (110) surface that provide definitive proof of the pure Yb divalency in YbB_6 [34], and, thus, additionally rule out these erroneous theory calculations.

A recent pressure dependent study of YbB_6 [33] observes key results of (i) no structural transition up to 30 GPa from x-ray diffraction, (ii) a rapid order-of-magnitude decrease in the resistivity up to 5 GPa, (iii) a pressure region of rather constant resistivity and Hall coefficient from 5–15 GPa, and (iv) a reemergence of thermally activated resistivity above 15 GPa accompanied by a small increase in Yb valency from pure divalency to 2.09+.

The theoretical calculation at 15 GPa in Fig. 4(b) shows a p-d overlap band structure and indicates that YbB_6 undergoes a semiconductor to semimetallic phase transition at an intermediate pressure. This occurs due to increase of p and d band widths and their wave function overlap. Such a p-d gap to p-d overlap transition naturally explains the rapid initial decrease in resistivity with pressure, also observed in early pressure-dependent transport of YbB_6 [63]. A semimetallic state in the intermediate 5–15 GPa pressure regime is also suggested by the nearly constant Hall coefficient, which is attributable to a balance between electron and hole carriers [33]. This transformation to semimetallic behavior under pressure provides a further confirmation of the existence of a semiconductor gap at ambient pressure where the ARPES experiments are performed.

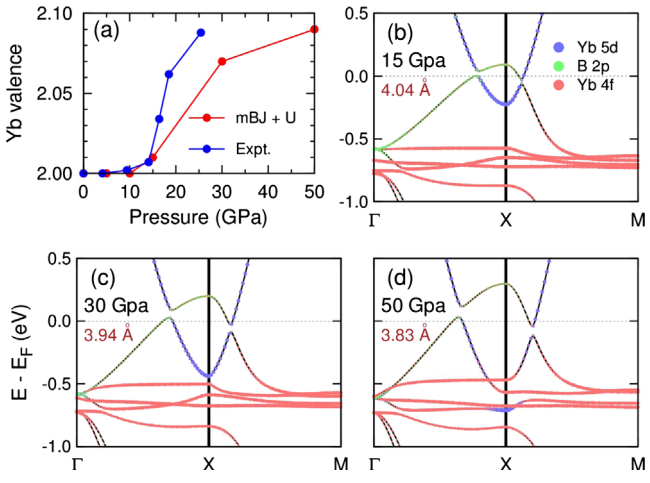

FIG. 4. (a) Pressure-dependent Yb valence state. For comparison, the experimental values are extracted from Ref. [33]. The mBJ + SOC + U (7 eV) band structures (b) under $P = 15$, (c) under $P = 30$, and (d) under $P = 50$ GPa.

The theoretical electronic structures for even greater pressures of 30 and 50 GPa in Figs. 4(c) and 4(d) show an increasing p-d overlap such that the Yb $4d$ band ultimately touches the Yb $4f$ band, which remains at nearly the same BE. The Yb $4f$ band exhibits only a small increase in bandwidth and slight centroid shift to lower BE but still remaining at the BE larger than 0.5 eV. Nevertheless, there is an increased mixing of Yb $4f$ character into the p states, as evidenced by the increasing band anticrossing gapping that results from the Yb $4f$ SOC interaction. The increasing Yb $4f$ character above E_F implies a decreased f occupation and mixed valency. Quantitative analysis of the Yb valence under pressure is plotted in Fig. 4(a). The resulting mixed valence, less than 10% at the highest pressure, compares favorably to the experimental results derived from Yb L_3 x-ray absorption measurements [33]. The experimental reemergence of a thermally activated resistivity ($dR/dT < 0$) above 15 GPa is plausibly due to the increasing $4f$ SOC-induced local gapping, whereas the overall resistivity rise due to gapping is weakened due to the competition of the increasing p-d overlap and hence increasing hole and electron FS volumes. The residual semimetallic conductivity can also explain the observed experimental low temperature resistivity plateaus [33].

This theoretical investigation allows us to comment generally on the feasibility of forming a TKI in actual materials. Since p-d states of opposite parity have inherently weak or negligible hybridization, the topologically nontrivial band inversion will have difficulty in forming a full insulator gap via hybridization alone. Therefore, some additional external influence is required to open up an insulating gap of sufficient size to practically realize in-gap topological surface states. Here, for the example of YbB_6 under pressure, the external influence is the hybridization mixing of the Yb $4f$ states with the p states and its larger $4f$ SOC-induced gapping. However this effect is still too small for YbB_6 to develop a full BZ p-d overlap gap at experimentally achievable pressures.

In conclusion, the flat-band conditions of the nonpolar (110) surface allow ARPES measurements to definitively show that YbB_6 is a non-Kondo non-TI semiconductor, and it opens up a new method for the quantitative characterization of the bulk gap of other divalent hexaborides. This result is in good agreement with predictions of theoretical

DFT + U calculations with proper treatment of $4f$ correlations and inclusion of well-established gap correction physics. Only under pressure does the topologically nontrivial p-d band inversion occur, but the system still retains a semimetallic electronic structure even up to high pressure beyond the onset of small Yb mixed valency.

This work was supported by the Korean NRF (No. 2011-0028736, No. 2013R1A1A2006416, No. 2014R1A1A2056546, No. 2015R1A2A1A15053564), Max-Plank POSTECH/KOREA Research Initiative (No. KR 2011-0031558), the KISTI supercomputing center (No. KSC-2015-C3-007), and the Deutsche Forschungsgemeinschaft via SFB 1170 (C06). Experiments were supported by the U.S. DOE at the Advanced Light Source (DE-AC02-05CH11231).

*jddenlinger@lbl.gov
†bimin@postech.ac.kr

[1] S. Raghu, X.-L. Qi, C. Honerkamp, and S.-C. Zhang, Phys. Rev. Lett. **100**, 156401 (2008).
[2] D. Pesin and L. Balents, Nat. Phys. **6**, 376 (2010).
[3] D. N. Sheng, Z.-C. Gu, K. Sun, and L. Sheng, Nat. Commun. **2**, 389 (2011).
[4] J. Maciejko and G. A. Fiete, Nat. Phys. **11**, 385 (2015).
[5] M. Dzero, K. Sun, V. Galitski, and P. Coleman, Phys. Rev. Lett. **104**, 106408 (2010).
[6] T. Takimoto, J. Phys. Soc. Jpn. **80**, 123710 (2011).
[7] M. Dzero, K. Sun, P. Coleman, and V. Galitski, Phys. Rev. B **85**, 045130 (2012).
[8] F. Lu, J.-Z. Zhao, H. Weng, Z. Fang, and X. Dai, Phys. Rev. Lett. **110**, 096401 (2013).
[9] S. Wolgast, Ç. Kurdak, K. Sun, J. W. Allen, D.-J. Kim, and Z. Fisk, Phys. Rev. B **88**, 180405(R) (2013).
[10] D. J. Kim, S. Thomas, T. Grant, J. Botimer, Z. Fisk, and J. Xia, Sci. Rep. **3**, 3150 (2013).
[11] D. J. Kim, J. Xia, and Z. Fisk, Nat. Mater. **13**, 466 (2014).
[12] J. D. Denlinger, J. W. Allen, J.-S. Kang, K. Sun, J.-W. Kim, J. H. Shim, B. I. Min, D.-J. Kim, and Z. Fisk, arXiv:1312.6637.
[13] M. Neupane, N. Alidoust, S.-Y. Xu, T. Kondo, Y. Ishida, D. J. Kim, C. Liu, I. Belopolski, Y. J. Jo, T.-R. Chang, H.-T. Jeng, T. Durakiewicz, L. Balicas, H. Lin, A. Bansil, S. Shin, Z. Fisk, and M. Z. Hasan, Nat. Commun. **4**, 2991 (2013).
[14] N. Xu, X. Shi, P. K. Biswas, C. E. Matt, R. S. Dhaka, Y. Huang, N. C. Plumb, M. Radović, J. H. Dil, E. Pomjakushina, K. Conder, A. Amato, Z. Salman, D. McK. Paul, J. Mesot, H. Ding, and M. Shi, Phys. Rev. B **88**, 121102(R) (2013).
[15] C.-H. Min, P. Lutz, S. Fiedler, B. Y. Kang, B. K. Cho, H.-D. Kim, H. Bentmann, and F. Reinert, Phys. Rev. Lett. **112**, 226402 (2014).
[16] M. M. Yee, Y. He, A. Soumyanarayanan, D.-J. Kim, Z. Fisk, and J. E. Hoffman, arXiv:1308.1085.
[17] S. Rössler, T.-H. Jang, D. J. Kim, L. H. Tjeng, Z. Fisk, F. Steglich, and S. Wirth, Proc. Natl. Acad. Sci. U.S.A. **111**, 4798 (2014).
[18] B. Yan, L. Müchler, X.-L. Qi, S.-C. Zhang, and C. Felser, Phys. Rev. B **85**, 165125 (2012).
[19] X. Zhang, H. Zhang, J. Wang, C. Felser, and S.-C. Zhang, Science **335**, 1464 (2012).
[20] X. Deng, K. Haule, and G. Kotliar, Phys. Rev. Lett. **111**, 176404 (2013).
[21] Z. Li, J. Li, P. Blaha, and N. Kioussis, Phys. Rev. B **89**, 121117(R) (2014).
[22] H. Weng, J. Zhao, Z. Wang, Z. Fang, and X. Dai, Phys. Rev. Lett. **112**, 016403 (2014).
[23] C.-J. Kang, H. C. Choi, K. Kim, and B. I. Min, Phys. Rev. Lett. **114**, 166404 (2015).
[24] D. Kasinathan, K. Koepernik, L. H. Tjeng, and M. W. Haverkort, Phys. Rev. B **91**, 195127 (2015).
[25] A. Kakizaki, A. Harasawa, T. Kinoshita, T. Ishii, T. Nanba, and S. Kunii, Physica (Amsterdam) **186–188B**, 80 (1993).
[26] M. Xia, J. Jiang, Z. R. Ye, Y. H. Wang, Y. Zhang, S. D. Chen, X. H. Niu, D. F. Xu, F. Chen, X. H. Chen, B. P. Xie, T. Zhang, and D. L. Feng, Sci. Rep. **4**, 5999 (2014).
[27] M. Neupane, S.-Y. Xu, N. Alidoust, G. Bian, D. J. Kim, C. Liu, I. Belopolski, T.-R. Chang, H.-T. Jeng, T. Durakiewicz, H. Lin, A. Bansil, Z. Fisk, and M. Z. Hasan, Phys. Rev. Lett. **114**, 016403 (2015).
[28] N. Xu, C. E. Matt, E. Pomjakushina, J. H. Dil, G. Landolt, J.-Z. Ma, X. Shi, R. S. Dhaka, N. C. Plumb, M. Radović, V. N. Strocov, T. K. Kim, M. Hoesch, K. Conder, J. Mesot, H. Ding, and M. Shi, arXiv:1405.0165.
[29] E. Frantzeskakis, N. de Jong, J. X. Zhang, X. Zhang, Z. Li, C. L. Liang, Y. Wang, A. Varykhalov, Y. K. Huang, and M. S. Golden, Phys. Rev. B **90**, 235116 (2014).
[30] T.-R. Chang, T. Das, P.-J. Chen, M. Neupane, S.-Y. Xu, M. Z. Hasan, H. Lin, H.-T. Jeng, and A. Bansil, Phys. Rev. B **91**, 155151 (2015).
[31] J. Jun, B. Jiang, and L. Lemin, J. Rare Earth **25**, 654 (2007).
[32] F. Tran and P. Blaha, Phys. Rev. Lett. **102**, 226401 (2009).
[33] Y. Zhou *et al.*, Phys. Rev. B **92**, 241118(R) (2015).
[34] See Supplemental Material at http://link.aps.org/supplemental/10.1103/PhysRevLett.116.116401, which includes Refs. [35–46], for the detailed ARPES data and DFT results for YbB_6, and the link between YbB_6 and SmB_6.
[35] T. Nanba, M. Tomikawa, Y. Mori, N. Shino, S. Imada, S. Suga, S. Kimura, and S. Kunii, Physica (Amsterdam) **186–188B**, 557 (1993).
[36] J. L. Gavilano, Sh. Mushkolaj, D. Rau, H. R. Ott, A. Bianchi, and Z. Fisk, Physica (Amsterdam) **329–333B**, 570 (2003).
[37] E. O. Kane, J. Phys. Chem. Solids **1**, 249 (1957).
[38] J. A. Lo'pez-Villanueva, I. Melchor, P. Cartujo, and J. E. Carceller, Phys. Rev. B **48**, 1626 (1993).
[39] G. Kresse and J. Furthmüller, Phys. Rev. B **54**, 11169 (1996); Comput. Mater. Sci. **6**, 15 (1996).
[40] G. K. H. Madsen and P. Novák, Europhys. Lett. **69**, 777 (2005).
[41] B. Lee and L.-W. Wang, Appl. Phys. Lett. **87**, 262509 (2005).
[42] Z.-H. Zhu, A. Nicolaou, G. Levy, N. P. Butch, P. Syers, X. F. Wang, J. Paglione, G. A. Sawatzky, I. S. Elfimov, and A. Damascelli, Phys. Rev. Lett. **111**, 216402 (2013).
[43] R. Monnier and B. Delley, Phys. Rev. B **70**, 193403 (2004).
[44] C.-J. Kang and B. I. Min (unpublished).
[45] J. D. Denlinger, Sooyoung Jang, G. Li, L. Chen, B. J. Lawson, T. Asaba, C. Tinsman, F. Yu, K. Sun, J. W. Allen,

C. Kurdak, D.-J. Kim, Z. Fisk, and Lu Li, arXiv:1601.07408.
[46] P. Hlawenka, K. Siemensmeyer, E. Weschke, A. Varykhalov, J. Sanchez-Barriga, N. Y. Shitsevalova, A. V. Dukhnenko, V. B. Filipov, S. Gabani, K. Flachbart, O. Rader, and E. D. L. Rienks, arXiv:1502.01542.
[47] P. Blaha, K. Schwarz, G. K. H. Madsen, D. Kvasnicka, and J. Luitz, *WIEN2k* (Karlheinz Schwarz, Techn. Universitat Wien, Austria, 2001).
[48] J. Kuneš and W. E. Pickett, Phys. Rev. B **69**, 165111 (2004).
[49] D. J. Singh, Phys. Rev. B **82**, 205102 (2010).
[50] J. D. Denlinger, APS March Meeting, 2015, http://meetings.aps.org/link/BAPS.2015.MAR.J10.13.
[51] J. M. Tarascon, J. Etourneau, P. Dordor, P. Hagenmuller, M. Kasaya, and J. M. D. Coey, J. Appl. Phys. **51**, 574 (1980).
[52] J. Y. Kim, N. H. Sung, and B. K. Cho, J. Appl. Phys. **101**, 09D512 (2007).
[53] G. Schönhense, Phys. Scr. **T31**, 255 (1990).
[54] Spin-resolved ARPES controversies are discussed in I. Gierz *et al.*, arXiv:1004.1573v2; C. Jozwiak *et al.*, Nat. Phys. **9**, 293 (2013); J. Sánchez-Barriga *et al.*, Phys. Rev. X **4**, 011046 (2014).
[55] In the presence of SOC, both *p*-*d* bands have the same symmetries, e.g., Δ_7 along Γ-X. But, without the SOC, they have different band symmetries, e.g., Δ_4 and Δ_3, respectively, and so no local anticrossing gap opens along Γ-X.
[56] S. Massidda, R. Monnier, and E. Stoll, Eur. Phys. J. B **17**, 645 (2000).
[57] A. Hasegawa and A. Yanase, J. Phys. C **12**, 5431 (1979).
[58] C. O. Rodriguez, R. Weht, and W. E. Pickett, Phys. Rev. Lett. **84**, 3903 (2000); **86**, 1142 (2001).
[59] H. J. Tromp, P. van Gelderen, P. J. Kelly, G. Brocks, and P. A. Bobbert, Phys. Rev. Lett. **87**, 016401 (2001).
[60] J. D. Denlinger, J. A. Clack, J. W. Allen, G.-H. Gweon, D. M. Poirier, C. G. Olson, J. L. Sarrao, A. D. Bianchi, and Z. Fisk, Phys. Rev. Lett. **89**, 157601 (2002).
[61] B. K. Cho, J.-S. Rhyee, B. H. Oh, M. H. Jung, H. C. Kim, Y. K. Yoon, J. H. Kim, and T. Ekino, Phys. Rev. B **69**, 113202 (2004).
[62] J.-S. Rhyee and B. K. Cho, J. Appl. Phys. **95**, 6675 (2004).
[63] V. A. Sidorov, N. N. Stepanov, O. B. Tsiok, L. G. Khvostantsev, I. A. Smirnov, and M. M. Korsukova, Sov. Phys. Solid State **33**, 720 (1991).